

Secretory Low Molecular Weight Phospholipase A₂ Plays Important Roles in Cell Elongation and Shoot Gravitropism in Arabidopsis

Hyoungh Yool Lee,^a Sung Chul Bahn,^b Yoon-Mi Kang,^a Kyu Hee Lee,^a Hae Jin Kim,^b Eun Kyeong Noh,^a Jiwan P. Palta,^c Jeong Sheop Shin,^{b,1} and Stephen B. Ryu^{a,1,2}

^a Kumho Life and Environmental Science Laboratory, Gwangju 500–712, Korea

^b Graduate School of Biotechnology, Korea University, Seoul 136–701, Korea

^c Department of Horticulture, University of Wisconsin-Madison, Madison, Wisconsin 53706

To elucidate the cellular functions of phospholipase A₂ in plants, an Arabidopsis cDNA encoding a secretory low molecular weight phospholipase A₂ (*AtsPLA₂β*) was isolated. Phenotype analyses of transgenic plants showed that overexpression of *AtsPLA₂β* promotes cell elongation, resulting in prolonged leaf petioles and inflorescence stems, whereas RNA interference-mediated silencing of *AtsPLA₂β* expression retards cell elongation, resulting in shortened leaf petioles and stems. *AtsPLA₂β* is expressed in the cortical, vascular, and endodermal cells of the actively growing tissues of inflorescence stems and hypocotyls. *AtsPLA₂β* then is secreted into the extracellular spaces, where signaling for cell wall acidification is thought to occur. *AtsPLA₂β*-overexpressing or -silenced transgenic plants showed altered gravitropism in inflorescence stems and hypocotyls. *AtsPLA₂β* expression is induced rapidly by auxin treatment and in the curving regions of inflorescence stems undergoing the gravitropic response. These results suggest that *AtsPLA₂β* regulates the process of cell elongation and plays important roles in shoot gravitropism by mediating auxin-induced cell elongation.

INTRODUCTION

Phospholipase A₂ (PLA₂) hydrolyzes glycerophospholipids at the *sn*-2 position to yield free fatty acids and lysophospholipids. PLA₂s have been implicated in diverse cellular responses in animal systems, including bioactive lipid production, host defense, and signal transduction (Li-Stiles et al., 1998; Zhang et al., 1999). PLA₂ activities also have been implicated in important cellular processes in plants, such as lipid metabolism (Chapman, 1998; May et al., 1998), defense signaling (Munnik et al., 1998; Roos et al., 1999), and auxin-stimulated cell growth (Scherer and Arnold, 1997; Paul et al., 1998). Auxin induces a rapid increase of free fatty acid (FFA), lysophosphatidylcholine (LPC), and lysophosphatidylethanolamine (LPE) levels in microsomes, which suggests that PLA₂ may be activated during auxin-stimulated cell growth (Scherer, 1996; Paul et al., 1998). Furthermore, the auxin-dependent elongation of hypocotyl segments is inhibited by treatment with PLA₂ inhibitors (Scherer and Arnold, 1997), suggesting that PLA₂ may be involved in auxin signaling leading to cell elongation.

The lysophospholipid LPE was found to retard senescence in leaves, flowers, and fruit (Farag and Palta, 1993a; Kaur and Palta, 1997) and to accelerate fruit ripening (Farag and Palta, 1993b) when applied as a spray. LPE inhibits phospholipase D, a key enzyme in promoting the membrane deterioration that leads to plant senescence (Ryu et al., 1997). PLA₂ also has been suggested to

be involved in plant defense responses to wound stress and pathogen elicitors (Creelman and Mullet, 1997; Lee et al., 1997; Chapman, 1998; Senda et al., 1998; Narváez-Vásquez et al., 1999). The activation of oxylipin-based chemical defenses in diatoms is initiated by PLA₂ activity (Pohnert, 2002). During embryo maturation, PLA-like activities have been implicated in the selective removal of unusual fatty acids from phospholipids in the endoplasmic reticulum for their reincorporation into triacylglycerols (Ståhl et al., 1995, 1998, 1999).

Despite the potentially significant physiological roles of PLA₂ in plants, little is known about the nature of plant secretory low molecular weight PLA₂ (sPLA₂) enzymes and genes. To date, sPLA₂ activity in plants has been demonstrated only in more or less purified preparations (Ståhl et al., 1998, 1999), and putative sPLA₂ genes were cloned recently from carnation and rice (Kim et al., 1999; Ståhl et al., 1999). A molecular understanding of these enzymes is necessary for the delineation of their cellular functions. To gain insight into the cellular functions of sPLA₂, we cloned a sPLA₂ gene from Arabidopsis (*AtsPLA₂β*) and generated transgenic Arabidopsis plants that silence *AtsPLA₂β* expression as a result of RNA interference (RNAi) or overexpress *AtsPLA₂β*. Here, we report that *AtsPLA₂β* plays important roles in cell elongation and shoot gravitropism in Arabidopsis.

RESULTS

Molecular Cloning and Sequence Analysis of Arabidopsis PLA₂ cDNA

Using the previously published N-terminal amino acid sequence of an elm PLA₂ (Ståhl et al., 1998) as a query, we identified and

¹ To whom correspondence should be addressed. E-mail sbryu@hanmail.net; fax 82-2-927-9028; or e-mail jsshin@korea.ac.kr; fax 82-2-927-9028.

² Current address: Graduate School of Biotechnology, Korea University, Seoul 136–701, Korea

Article, publication date, and citation information can be found at www.plantcell.org/cgi/doi/10.1105/tpc.014423.

cloned an Arabidopsis sPLA₂ cDNA. AtsPLA₂β is located on the long arm of chromosome II and is registered as a hypothetical protein (At2g19690). We found that its coding region was predicted incorrectly and have registered the correct cDNA nucleotide sequence with the National Center for Biotechnology Information. The deduced amino acid sequence of the encoded AtsPLA₂β protein is shown in Figure 1. The 590-bp clone includes a 441-bp open reading frame between nucleotides 20 and 459, which encodes a protein of 147 amino acids with a predicted molecular weight of 16,288 and a pI of 8.23 (Figure 1).

Sequence analysis revealed that AtsPLA₂β contains catalytic motif sequences identified in animal sPLA₂s, such as the Ca²⁺ binding loop and active site (Figure 1) (White et al., 1990). The active site motif of AtsPLA₂β contains a well-conserved His/Asp dyad (Figure 1), indicating that AtsPLA₂β belongs to a class of PLA₂ proteins that use a catalytic His according to Six and Dennis (2000). Disulfide bridges are important for PLA₂ protein stability; the number of bridges is used as a criterion to classify animal PLA₂s. The AtsPLA₂β amino acid sequence includes 12 Cys residues that potentially can form six intramolecular disulfide bridges. Seven of the 12 Cys residues in AtsPLA₂β align well with Cys in cobra venom sPLA₂ (Figure 1).

Of the putative plant sPLA₂s that have been reported, AtsPLA₂β shares overall amino acid identities of 46, 30, and 28% with rice sPLA₂ isoform I, rice sPLA₂ isoform II, and carnation sPLA₂, respectively. However, in a 33-amino acid sequence that contains the catalytic motifs, the identity becomes 84, 81, and 75%, respectively. This result indicates that AtsPLA₂β is related most closely to the putative rice sPLA₂ isoform I.

Signal Peptide and the Mature Form of AtsPLA₂β Expressed in *Escherichia coli*

Sequence analysis using the pSORT program (<http://psort.nibb.ac.jp.ggoa/>) predicted that AtsPLA₂β, like animal sPLA₂s, has a potential N-terminal signal peptide (Figure 1). The predicted cleavage site of the signal peptide lies between Ser-28 and Glu-29, which would result in a mature protein of 119 amino acids. A fusion protein (DsbC-sPLA₂) containing the mature form of AtsPLA₂β was produced in *E. coli* and purified from the resulting cell-free extract (Figure 2A). The free mature AtsPLA₂β protein was purified after enzymatic dissociation from the DsbC fusion protein and purification (Figure 2A, lane 2). The molecular mass of mature AtsPLA₂β was ~13 kD, which is in good agreement with the calculated molecular mass of 13.2 kD (pI = 7.7).

Functional Analysis of Recombinant AtsPLA₂β

To determine if the recombinant protein is functional, both the unprocessed and mature forms of AtsPLA₂β were tested for enzymatic activity. The fusion protein containing AtsPLA₂β was capable of hydrolyzing the substrate phosphatidylcholine (PC) into two products that comigrate with the LPC and FFA standards (Figure 2B, lanes 3 and 4). Commercial snake venom sPLA₂ completely hydrolyzed the substrate into the same products (Figure 2B, lane 1), whereas the protein DsbC alone exhibited only background levels of hydrolysis activity (Figure 2B, lane 2). The specific activity of the free mature form of AtsPLA₂β was determined to be 530 nmol·min⁻¹·mg⁻¹ protein, which is

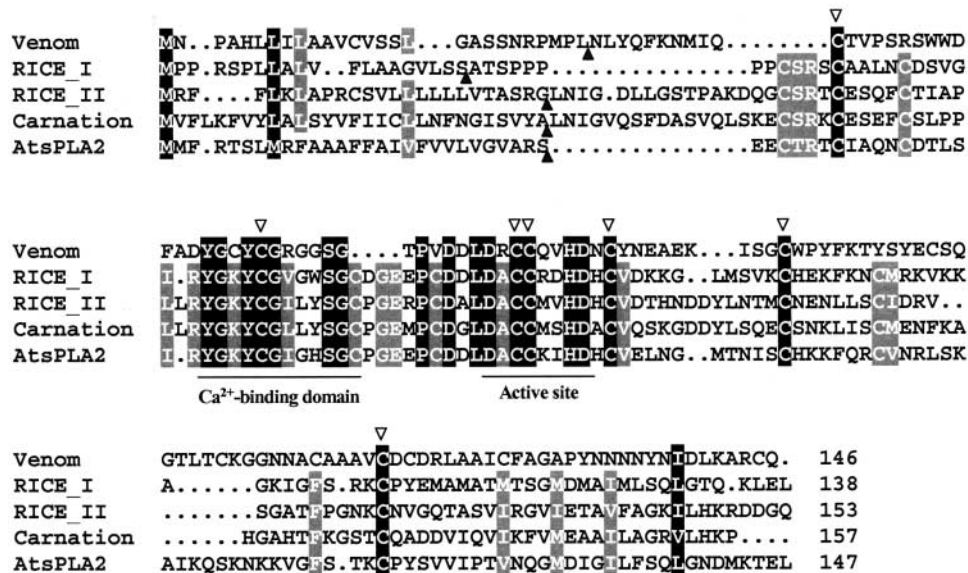


Figure 1. Amino Acid Sequence Comparison of AtsPLA₂β with Other Plant sPLA₂s and Snake Venom sPLA₂ (Group IA).

The cleavage sites for the removal of N-terminal signal peptides as predicted by the pSORT program are indicated by closed triangles. Residues that are conserved completely among the five sequences are indicated by black boxes, and partially conserved residues are indicated by gray boxes. The Ca²⁺ binding domain and the active site motif of animal sPLA₂s and the corresponding domain sequences in the plant sPLA₂s are underlined. The Cys residues that are conserved completely between venom sPLA₂, AtsPLA₂β, and the three putative plant sPLA₂s are indicated by open triangles.

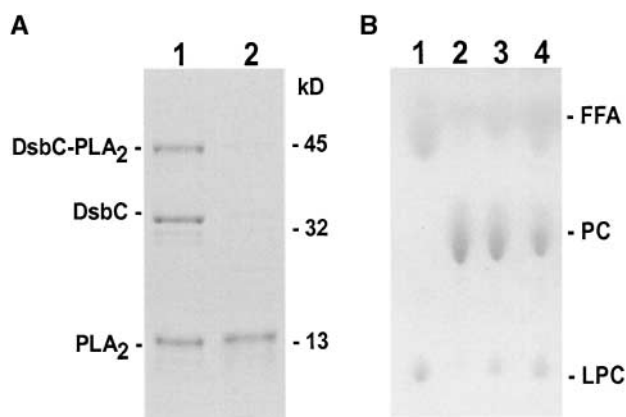


Figure 2. Production of Recombinant *AtsPLA₂β* and Thin Layer Chromatography Analysis of Its Hydrolytic Activity.

(A) Recombinant mature *AtsPLA₂β* proteins were separated by 12% SDS-PAGE and stained with Coomassie blue. Lane 1, DsbC-*AtsPLA₂β* fusion proteins purified from crude extracts of recombinant *E. coli* and digested with the enzyme rEK; lane 2, free mature form of *AtsPLA₂β* isolated from the mixture shown in lane 1 with the S-Tag rEK purification kit. **(B)** Thin layer chromatography analysis of the hydrolytic activity of recombinant *AtsPLA₂β*. The substrate PC is hydrolyzed into LPC and FFA by *PLA₂* activity. Lane 1, snake venom s*PLA₂*; lane 2, DsbC purified from *E. coli* transformed with the vector pET40; lanes 3 and 4, DsbC-*AtsPLA₂β* fusion proteins purified from *E. coli* transformed with pET40 containing the full-length *AtsPLA₂β* cDNA. The total amount of protein loaded in lane 4 was twice the amount loaded in lane 3.

twice as great as that of its free unprocessed form. The free mature form of *AtsPLA₂β* still was active after 5 min of boiling treatment but lost 37% of its original activity after treatment with 5 mM DTT.

The specificity of *AtsPLA₂β* with respect to the *sn* position in PC was determined by incubating the free mature form with three different substrates (Table 1). Radioactive LPC was not detected among reaction products when the protein was incubated with 1-palmitoyl-2-¹⁴C-palmitoyl-PC or 1-palmitoyl-2-¹⁴C-linoleoyl-PC, indicating that the enzyme does not act at the *sn*-1 position of PC (Table 1). When 1,2-¹⁴C-dipalmitoyl-PC was used as a substrate, similar levels of radioactive carbon were measured in the LPC and FFA spots. These results suggest that *AtsPLA₂β* catalyzes hydrolysis at the *sn*-2 position; therefore, it is a *PLA₂* and not a *PLA₁* enzyme. At the *sn*-2 position, *AtsPLA₂β* protein hydrolyzed palmitoyl acyl chains at a higher rate than linoleoyl acyl chains (Table 1).

Tissue-Specific and Auxin-Induced Expression of the *AtsPLA₂β* Transcript

To investigate the expression of the *AtsPLA₂β* gene in different plant organs, we isolated total RNA from Arabidopsis roots, stems, leaves, flowers, and siliques. Because we were unable to detect s*PLA₂* transcripts in any of these tissues by RNA gel blot analysis (data not shown), we used quantitative reverse transcriptase-mediated (RT) PCR to amplify cDNA from low-abundance s*PLA₂* mRNA. The concomitant amplification of an 18S

rRNA served as an internal standard. The ratio 1:9 (rRNA primer: competitor) allowed nearly equal amplification of s*PLA₂* cDNA and rRNA cDNA (Figure 3A, top gels), indicating that *AtsPLA₂β* transcripts are extremely rare. *AtsPLA₂β* transcripts were detected at similar levels in Arabidopsis roots, stems, leaves, and siliques but at higher levels in flowers (Figure 3A, top). The *AtsPLA₂β* transcription levels also depended on the developmental stage (Figure 3A, bottom gels). A higher level of *AtsPLA₂β* expression was detected in open flowers than in unopened flowers, and cotyledons expressed more transcripts than the primary and secondary leaf tissues. We also examined whether the expression of the *AtsPLA₂β* gene is responsive to auxin. Both RNA gel blot and RT-PCR analyses showed that *AtsPLA₂β* expression was induced rapidly after treatment with 20 μM indoleacetic acid (Figure 3B). An increase in the amount of *AtsPLA₂β* transcripts was detected within 30 min. Using 18S and ubiquitin levels as references, the results of RNA gel blot and RT-PCR analyses indicated that the induction of *AtsPLA₂β* transcripts peaked after 1 to 1.5 h and remained steady over the 4-h auxin treatment (Figure 3B).

The tissue- and developmental stage-specific profile of the *AtsPLA₂β* promoter activity was investigated using histochemical β-glucuronidase (GUS) assays. GUS activity was present in all tissues at the actively growing young stages of Arabidopsis seedlings (Figure 4A). When plants grew, however, *AtsPLA₂β* expression was evident only in cotyledons, primary leaves, and hypocotyls (Figures 4B and 4C). The activity decreased in the secondary leaves, being detectable only in vascular tissues (Figure 4C). In the roots as well, expression was localized mostly in vascular tissues (Figures 4B and 4H). *AtsPLA₂β* expression became highly active when floral shoots bolted, especially in the young or actively growing tissues of inflorescence stems (Figure 4D). *AtsPLA₂β* promoter activity gradually was stimulated in opening flowers (Figures 4E and 4F), as shown by RT-PCR analysis (Figure 3A, bottom gels). In the full open floral tissues, expression was high in the filaments, styles, sepals, and pedicels but low or undetectable in petals, anthers, stigmas, and ovaries (Figure 4F). In the siliques, GUS staining was observed in the carpels, false septa, and pedicels but not in the maturing seeds (Figure 4G). Cross-sectional analyses showed strong *AtsPLA₂β* promoter activity in the cortical, vascular, and endodermal tissues of inflorescence stems and hypocotyls (Figures 4I and 4J), but *AtsPLA₂β* expression in the root was localized in the vascular tissues (Figure 4K).

Table 1. *sn* Specificity and Acyl Preference of the *E. coli*-Expressed Mature Enzyme of *AtsPLA₂β* for the Substrate PC

Substrate	Percent of Input ¹⁴ C Recovered as	
	LPC	FFA
1-Palmitoyl-2- ¹⁴ C-palmitoyl-PC	1.90 ± 0.10	73.40 ± 1.75
1-Palmitoyl-2- ¹⁴ C-linoleoyl-PC	1.50 ± 1.20	62.20 ± 2.20
1,2- ¹⁴ C-Dipalmitoyl-PC	34.60 ± 0.10	48.70 ± 0.29

Values shown are means ± SE obtained from three independent in vitro assays (*n* = 3).

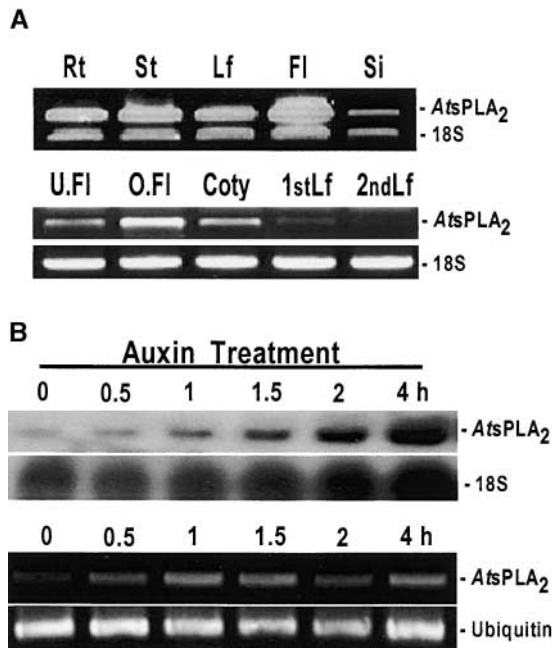


Figure 3. Tissue-Specific and Auxin-Induced Expression of *AtsPLA₂β* Transcripts.

(A) The top gel shows tissue-specific expression. Total RNA was isolated from the root (Rt), stem (St), leaf (Lf), flower (Fl), and silique (Si) tissues of 5-week-old plants, reverse transcribed, and used as the template for PCR with primers that amplify a 436-bp *AtsPLA₂β* fragment and a 315-bp 18S rRNA fragment. The primers used to amplify the 18S fragment were a mixture of 18S primers and 18S competitors (1:9, v/v). Thirty-five cycles of RT-PCR were used to amplify both *AtsPLA₂β* and 18S rRNA fragments. The bottom gels show developmental stage-specific expression. Total RNA was isolated from unopened flowers (U.FI) and opened flowers (O.FI) of 5-week-old plants and from cotyledons (Coty), primary leaves (1stLf), and secondary leaves (2ndLf) of 2-week-old plants. Thirty-five cycles of RT-PCR were used to amplify *AtsPLA₂β*, and 20 cycles were used to amplify 18S fragments with 18S primers without 18S competitors.

(B) The top gels show RNA gel blot results. Total RNA was extracted from 10-day-old seedlings in a Petri dish at 0, 0.5, 1, 1.5, 2, and 4 h after treatment with 20 μM indoleacetic acid. The blot membrane with the *AtsPLA₂β* probe was exposed to x-ray film for 15 days, and the blot membrane with the 18S rRNA probe was exposed for 1 day. The bottom gels show RT-PCR results with mRNA isolated from total RNA. Twenty-nine and 20 cycles of RT-PCR were used to amplify *AtsPLA₂β* and ubiquitin fragments, respectively.

AtsPLA₂β Is Secreted into Cell Wall/Extracellular Spaces

The identification of a putative signal peptide in *AtsPLA₂β* indicates that, like animal sPLA₂s, the enzyme is likely to be a secreted protein. Computer analysis with the pSORT program predicted that *AtsPLA₂β* is located in the cell wall/extracellular space (certainty = 0.82) and in the vacuole (certainty = 0.41). To determine experimentally the subcellular localization of *AtsPLA₂β*, we introduced vector constructs encoding *AtsPLA₂β*-green fluorescent protein (GFP) fusion proteins into onion epidermal cells. In these vector constructs, GFP was fused either to the C

terminus of *AtsPLA₂β* or to the putative signal peptide alone, as indicated in Figure 5. Although the GFP control localized inside the cytoplasm (Figure 5A), the *AtsPLA₂β*-GFP fusion protein accumulated densely in the interstices of the cell wall/extracellular space (Figure 5B). The signal peptide-GFP fusion protein also was observed in the intercellular space (Figure 5C), but with a more diffuse distribution compared with that of the *AtsPLA₂β*-GFP fusion protein. This is probably the result of the high mobility of the soluble GFP protein after dissociation from the signal peptide during secretion. These observations suggest that expressed *AtsPLA₂β* protein is secreted into the cell wall/extracellular space and that the secretion of the protein is mediated by the signal peptide.

Upregulation or Downregulation of *AtsPLA₂β* Expression Alters Shoot Gravitropism

To gain further insights into the cellular functions of *AtsPLA₂β*, we generated transgenic Arabidopsis plants (ecotype Columbia [Col-0]) that overexpress *AtsPLA₂β* or suppress *AtsPLA₂β* expression as a result of RNAi-mediated silencing. In three independent *AtsPLA₂β*-overexpressing and three independent *AtsPLA₂β*-silenced T3 transgenic lines, RT-PCR and PLA₂ activity assays demonstrated increased and reduced levels of gene expression and enzyme activity, respectively, compared with wild-type plants (Figures 6A and 6B). The inflorescence stems of wild-type and *AtsPLA₂β*-overexpressing transgenic plants were analyzed for gravitropic responses (Figures 6C to 6F). After being placed horizontally, wild-type stems began to bend upward, curving >100° within 60 min, which is indicative of a strong negative gravitropic response (Figure 6C). By contrast, transgenic Arabidopsis plants constitutively expressing *AtsPLA₂β* greatly reduced gravitropic responses (Figures 6D to 6F), whereas the plants transformed with the vector pBI121 showed gravitropic responses similar to those of wild-type plants (data not shown). Over the course of time (Figure 7A), the stems of transgenic plants constitutively expressing *AtsPLA₂β* showed a significantly slower gravitropic response. Although wild-type stems bent by ~50° at 30 min after gravistimulation, the stems of plants overexpressing *AtsPLA₂β* showed little response (Figure 7A). Wild-type stems curved up to 125° from 90 to 120 min. After 2 h, they began to curve back, defining a final angle of 90° by 3 h. The stems of *AtsPLA₂β*-overexpressing plants bent by 90° within 90 min but did not bend further (Figure 7A). Hence, from 3 h after gravistimulation, the stems of both wild-type and transgenic plants resumed vertical growth (Figure 7A).

The hypocotyls of transgenic Arabidopsis seedlings that overexpress *AtsPLA₂β* or suppress *AtsPLA₂β* expression as a result of RNAi-mediated silencing also showed altered gravitropic responses compared with wild-type plants (Figures 6G to 6L). Although the hypocotyls of wild-type plants had bent almost vertically at 26 h after horizontal gravistimulation, the hypocotyls of *AtsPLA₂β*-overexpressing or -silenced transgenic seedlings showed significantly slower gravitropic responses (Table 2). However, the roots of the transgenic seedlings showed more or less similar gravitropic responses to wild-type roots (Table 2).

We investigated whether *AtsPLA₂β* promoter activity is induced during the gravitropic response of the florescence stems

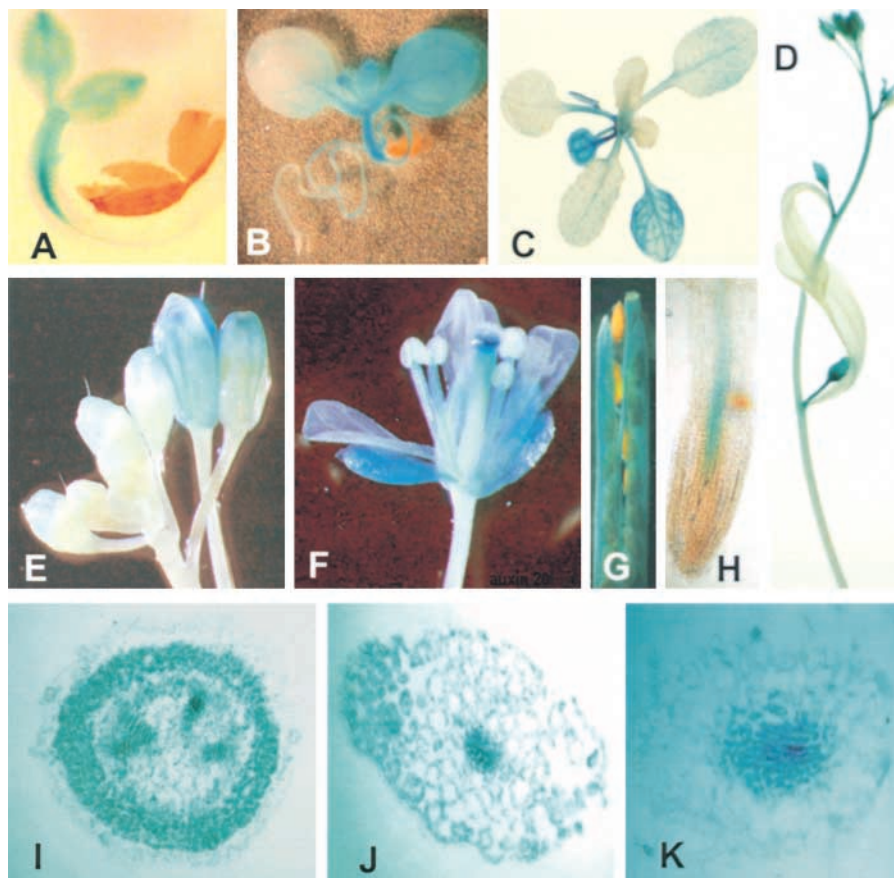


Figure 4. Histochemical Localization of GUS Activity in Arabidopsis (Col-0) Plants Transformed with the *AtsPLA₂β* Promoter-GUS Construct.

- (A) A 2-day-old seedling.
 (B) A 6-day-old seedling.
 (C) A 3-week-old plant.
 (D) Inflorescence stems from a 4-week-old plant.
 (E) and (F) Floral tissues from a 5-week-old plant.
 (G) Silique tissues from a 6-week-old plant.
 (H) Roots from a 4-week-old plant.
 (I) Cross-section of the young inflorescence stem of a 5-week-old plant.
 (J) Cross-section of the hypocotyl of a 10-day-old plant.
 (K) Cross-section of the main root of a 2-week-old plant.

using GUS assays. Strong GUS activity was observed in the curving regions of inflorescence stems undergoing the gravitropic response, indicating gravitropic response-specific activation of the *AtsPLA₂β* promoter (Figure 7B).

Cell Elongation Rates Are Altered in Leaf Petioles and Inflorescence Stems of Transgenic Plants

Leaf petiole lengths and leaf sizes were enlarged (~40 to 45%) in *AtsPLA₂β*-overexpressing transgenic plants and reduced (~20 to 30%) in *AtsPLA₂β*-silenced transgenic plants compared with wild-type plants (Figures 8A and 8B). To determine whether the alterations in leaf size and petiole length in the transgenic plants resulted from different levels of cell division and/or cell elongation, we measured the sizes of epidermal and

cortical cells by light microscopy. The epidermal and cortical cells were significantly longer longitudinally (~40 to 50%) in *AtsPLA₂β*-overexpressing transgenic plants and significantly shorter (~30 to 45%) in *AtsPLA₂β*-silenced plants compared with wild-type plants (Figure 8C, Table 3). Because cell elongation levels reflect well the differences in petiole lengths between wild-type and *AtsPLA₂β*-overexpressing transgenic plants, the difference likely is attributable mainly to the different levels of cell elongation. In *AtsPLA₂β*-silenced transgenic plants, however, the degree of cell elongation decreased more than the degree of petiole length, suggesting that the shortened cell lengths might be compensated for, in part, by other factors such as cell division.

Transgenic plants overexpressing *AtsPLA₂β* also exhibited greater inflorescence stem elongation, whereas transgenic

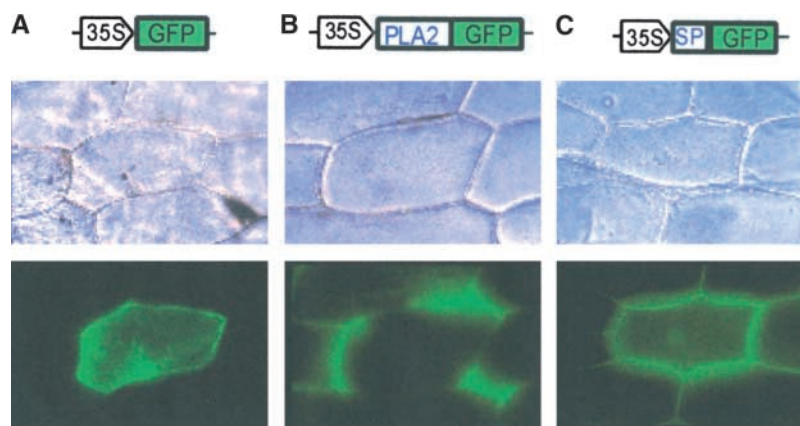


Figure 5. Subcellular Localization of *AtsPLA*₂ β Proteins.

GFP fusion constructs under the control of the 35S promoter of *Cauliflower mosaic virus* were introduced into onion epidermal cells by particle bombardment. A construct encoding only GFP was used as a control (**A**). GFP was fused in-frame to the C terminus of the full open reading frame of *AtsPLA*₂ β (**B**) or to the C terminus of the signal peptide sequence of *AtsPLA*₂ β (**C**). The top row depicts vector fusion constructs, the middle row depicts the onion cell structure observed by light microscopy, and the bottom row depicts the cytolocalization of GFP and GFP fusion proteins observed by fluorescence microscopy.

plants with silenced *AtsPLA*₂ β expression showed retarded stem elongation compared with wild-type plants, although the developmental stages of inflorescence stems were not significantly different among wild-type and transgenic plants (Figure 8A). Microscopic analysis demonstrated that the epidermal and cortical cells in the actively growing zone of stems also were longitudinally longer in *AtsPLA*₂ β -overexpressing plants and shorter in *AtsPLA*₂ β -silenced transgenic plants compared with wild-type plants (Table 3). The difference in inflorescence stem lengths among wild-type and transgenic plants was diminished at the geometrical growth stages \sim 10 days after bolting (Figure 9). These results suggest that the transient alterations in stem elongation result from differences in cell elongation rates and that *AtsPLA*₂ β plays important roles in the cellular process of cell elongation.

DISCUSSION

We have identified an Arabidopsis cDNA encoding a sPLA₂. The molecular mass of the mature form was calculated to be 13.2 kD, with a pI of 7.7. Although *AtsPLA*₂ β shares low overall amino acid identity (13 to 17%) with animal sPLA₂s, catalytic motif regions of the protein—the Ca²⁺ binding loop and the active site—show greater identity (up to 55%). According to the criteria established for animal sPLA₂s (Six and Dennis, 2000), *AtsPLA*₂ β is classified as a group-XI PLA₂.

Several putative sPLA₂ cDNAs have been cloned from the developing flowers of carnation and from rice (Kim et al., 1999; Ståhl et al., 1999). A Basic Local Alignment Search Tool (BLAST) search revealed that *AtsPLA*₂ β also shares sequence identity with other putative sPLA₂ cDNAs from *Populus*, tomato, cotton, pine, soybean, and rice. It is worth noting that a full search of the Arabidopsis genome identified multiple sPLA₂ genes (*At2g06925*, *At4g29460*, and *At4g29470*, which we named *AtsPLA*₂ α , *AtsPLA*₂ γ , and *AtsPLA*₂ δ , respectively). All of the pu-

tative enzymes encoded by these genes contain 12 conserved Cys residues, the highly conserved Ca²⁺ binding loop, and the active site motif. *AtsPLA*₂ β shares 31 to 57% overall identity with these Arabidopsis isoforms.

The 12 Cys residues in the mature *AtsPLA*₂ β protein may form six disulfide bonds, and the positions of these residues in *AtsPLA*₂ β are well conserved among plant sPLA₂s. Most animal sPLA₂s have six or seven disulfide bonds, although some have five or eight (Six and Dennis, 2000). The positioning of the Cys residues is partially conserved in spite of very low overall sequence identity. The Cys residues are known to play a critical role in the structural stability and enzymatic activity of animal sPLA₂s (Six and Dennis, 2000; Valentin and Lambeau, 2000). *AtsPLA*₂ β was stable even after 5 min of boiling, but its activity decreased significantly upon treatment with a reducing agent.

Previous studies of animal sPLA₂s have shown that the hydrolysis of phospholipids proceeds through the activation and coordination of a water molecule by hydrogen bonding to the active site His (Scott et al., 1990; Six and Dennis, 2000). An Asp residue provides the ligand for a crucial Ca²⁺ ion in forming a positively charged oxy-anion hole, stabilizing the negatively charged transition state of the PLA₂ reaction. *AtsPLA*₂ β also contains the well-conserved His/Asp dyad and therefore belongs to the subgroup of PLA₂s that use a catalytic His. Other conserved residues that are known to participate in hydrogen bonding networks, Tyr and Gly, also are found in the *AtsPLA*₂ β Ca²⁺ binding loop.

An acyl preference was observed for *AtsPLA*₂ β . *AtsPLA*₂ β hydrolyzed palmitoyl groups at a somewhat higher rate than linoleoyl groups. This property is distinct from that of developing elm seed sPLA₂, which showed a preference for caproyl and oleoyl groups (Ståhl et al., 1998). The nucleotide sequence of the elm seed sPLA₂ has not been determined, but the N-terminal amino acid sequence shares low identity (42%) with that of *AtsPLA*₂ β . Because *AtsPLA*₂ β is expressed predominantly in

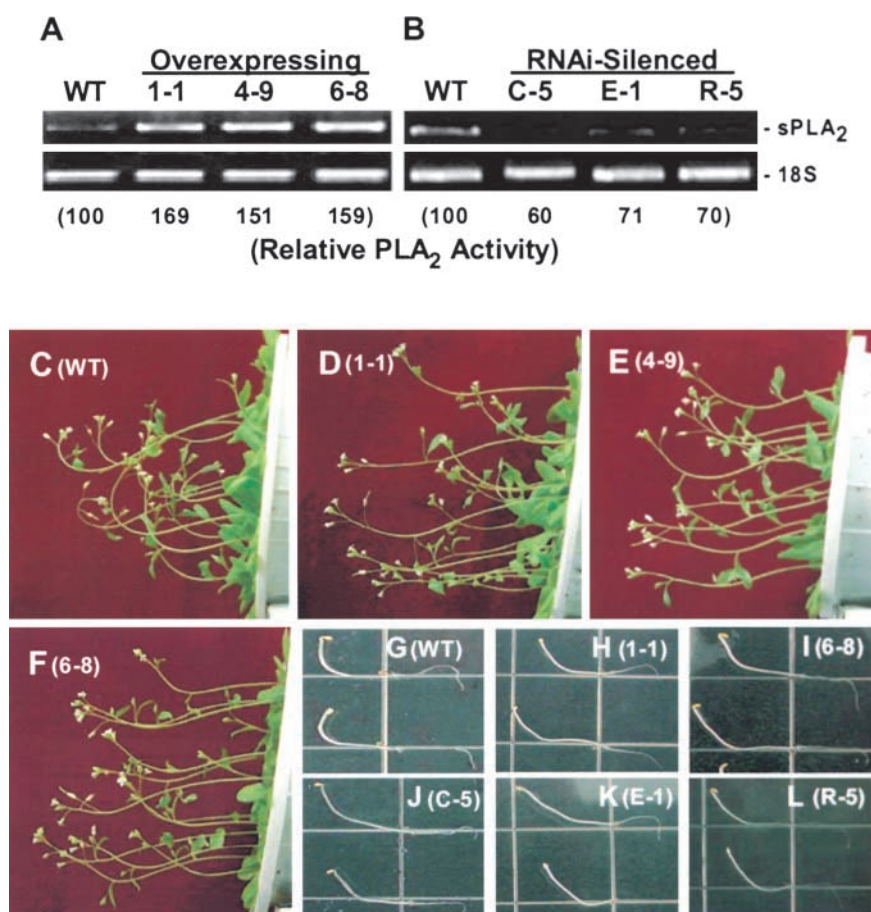


Figure 6. Gravitropic Responses of the Inflorescence Stems, Hypocotyls, and Roots of Transgenic Arabidopsis Plants (Col-0) That Overexpress *AtsPLA₂β* or Silence *AtsPLA₂β* Expression as a Result of RNAi Compared with Wild-Type Plants.

(A) and **(B)** Relative RT-PCR and PLA₂ activity in the inflorescence stems of three 5-week-old independent T3 transgenic Arabidopsis lines that overexpress *AtsPLA₂β* **(A)** and in the leaf tissues of three 2-week-old independent T3 transgenic Arabidopsis lines that suppress *AtsPLA₂β* expression as a result of RNAi **(B)**. Thirty-five and 20 cycles of RT-PCR were used to amplify *AtsPLA₂β* and 18S rRNA fragments, respectively. WT, wild type.

(C) to **(F)** Gravitropic responses of the inflorescence stems of 5-week-old wild-type plants **(C)** and three independent T3 transgenic lines overexpressing *AtsPLA₂β* **(D)** to **(F)** after 60 min of horizontal gravistimulation.

(G) to **(L)** Gravitropic responses of the hypocotyls and roots of 3-day-old dark-grown wild-type plants **(G)**, two independent T3 transgenic lines that overexpress *AtsPLA₂β* **(H)** and **(I)**, and three independent T3 transgenic lines that suppress *AtsPLA₂β* expression as a result of RNAi **(J)** to **(L)** after 26 h of horizontal gravistimulation.

actively growing young seedlings and floral organs, these two sPLA₂s may play distinctly different roles. The elm seed sPLA₂ was suggested to be involved in the removal of unusual fatty acids from membrane lipids (Ståhl et al., 1998).

Although little is known about the distribution and functions of sPLA₂s in plants (Ståhl et al., 1998, 1999), accumulating biochemical evidence suggests that plant PLA₂s are implicated in many important cellular activities, including auxin-stimulated cell growth (Paul et al., 1998). *AtsPLA₂β* is tissue- and developmental stage-specifically expressed at very low levels in plant tissues. Relatively strong activities of the *AtsPLA₂β* promoter were observed in all tissues at the stages of young seedling growth. As plants grew, however, expression gradually decreased in the primary and secondary leaves compared with that in the cotyledons. *AtsPLA₂β*

promoter activity was stimulated greatly after floral shoots had bolted, especially in young or actively growing inflorescence stem tissues and open flowers. In the open flowers, expression was detected in floral organs such as the filaments, sepals, and pedicels but was low or undetectable in petals, anthers, stigmas, ovaries, and maturing seeds. The *AtsPLA₂β* promoter activity in different tissues and at different stages of growth was consistent with the results of RT-PCR assays. Interestingly, gene expression of *AtsPLA₂β* was induced rapidly by auxin treatment within 30 min, suggesting that *AtsPLA₂β* may function as a mediator of auxin signaling in response to external stimuli. Because in *in vitro* assays, time is required for auxin transport into the tissues, we assume that the induction of *AtsPLA₂β* gene expression by endogenous auxin *in vivo* can be faster than that *in vitro*.

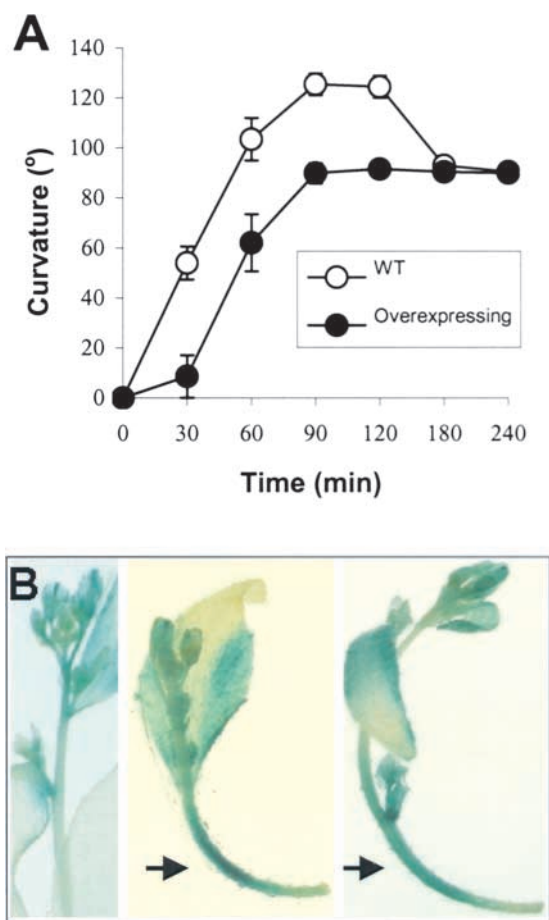


Figure 7. Time Course of the Gravitropic Response of the Inflorescence Stems of Wild-Type and Transgenic Arabidopsis Plants, and Gravitropic Response-Specific Activation of the *AtsPLA₂β* Promoter in the Curving Regions of Inflorescence Stems.

(A) Data for wild-type (WT) plants (Col-0; open circles) and *AtsPLA₂β*-overexpressing transgenic plants (T3 1-1 line; closed circles). Approximately 30 individual inflorescence stems were examined in each of four independent experiments. The vertical error bars represent SE values.

(B) Histochemical staining in the inflorescence stems of transgenic Arabidopsis (Col-0) carrying the *AtsPLA₂β* promoter-GUS construct at different stages of the gravitropic response. A control stem without gravistimulation (left) and stems with curvatures of 80° (middle) and 125° (right) are shown. The curving regions of the stems with strong GUS activity are indicated with arrows.

What is the role of *AtsPLA₂β* in the growth and development of Arabidopsis? The high levels of *AtsPLA₂β* transcript in actively growing cells suggest that *AtsPLA₂β* functions in cell growth and proliferation. Indeed, transgenic plants overexpressing *AtsPLA₂β* had prolonged leaf petioles and transiently more elongated inflorescence stems than did wild-type plants. By contrast, *AtsPLA₂β*-silenced transgenic plants had shortened leaf petioles and transiently less elongated inflorescence stems. Because the elongation of stems and petioles is dependent on cell division and/or cell elongation, we measured and compared the longitudinal lengths of the epidermal and cortical cells of the petioles and stems of transgenic and wild-type plants. Cell elongation levels were significantly different among the transgenic and wild-type plants and clearly were related to the differences in petiole and stem lengths. These results suggest that the overexpression of *AtsPLA₂β* promotes cell elongation, resulting in prolonged leaf petioles and inflorescence stems, whereas suppression of *AtsPLA₂β* retards cell elongation, resulting in shortened leaf petioles and inflorescence stems.

These results are consistent with previously reported observations. The *in vitro* addition of the *PLA₂* enzyme products LPC and linolenic acid accelerates the elongation of maize coleoptile segments (Yi et al., 1996). Treatment of oat roots with exogenous *PLA₂* or with the enzyme products stimulates H⁺ pump activity in plasma membrane vesicles (Palmgren and Sommarin, 1989). The acidification of cell walls by the activation of H⁺ pumps appears to be mediated by the lysophospholipid-induced activation of protein kinase (Martiny-Baron and Scherer, 1989). In addition, LPC activates NADH oxidase, an enzyme that is involved directly in cell elongation (Brightman et al., 1991). The previously reported evidence and our results lead us to propose the role of *AtsPLA₂β* in mediating cell elongation. *AtsPLA₂β* is expressed in actively growing stem tissues and secreted into the extracellular space. *AtsPLA₂β* activity yields its enzymatic products, lysophospholipids and FFAs, by hydrolyzing cell membrane phospholipids. The enzymatic products may stimulate H⁺ pumps so that the cell wall is acidified and also may activate other enzymes involved directly in cell elongation, including certain protein kinases.

Auxin-induced differential stem elongation has long been suggested to play a major role in the gravitropic response of plants (Kiss, 2000; Kato et al., 2002; Moore, 2002). To determine whether *AtsPLA₂β* is involved in the gravitropic response, the inflorescence stems of wild-type and *AtsPLA₂β*-overexpressing transgenic Arabidopsis plants were placed horizontally. The rates of gravitropic

Table 2. Gravitropic Responses of the Hypocotyls and Roots of Transgenic Arabidopsis Plants That Overexpress *AtsPLA₂β* or Silence *AtsPLA₂β* Expression Compared with Wild-Type Plants

Organ	Wild Type	Overexpressing		RNAi Silenced		
		1-1	6-19	C-5	E-1	R-5
Hypocotyl	88.8 ± 1.8	74.3 ± 1.3 ^a	68.0 ± 4.0 ^b	67.5 ± 5.3 ^b	68.0 ± 3.0 ^b	69.0 ± 1.0 ^b
Root	76.4 ± 2.2	69.9 ± 2.3	76.1 ± 1.0	84.3 ± 1.2	78.7 ± 5.8	74.5 ± 1.7

Values shown are mean curvature degrees ± SE obtained from three independent experiments (*n* = 60). Data were collected 26 h after horizontal gravistimulation.

^a Mean values are statistically different (*P* < 0.005) from mean values in the wild type.

^b Mean values are statistically different (*P* < 0.001) from mean values in the wild type.

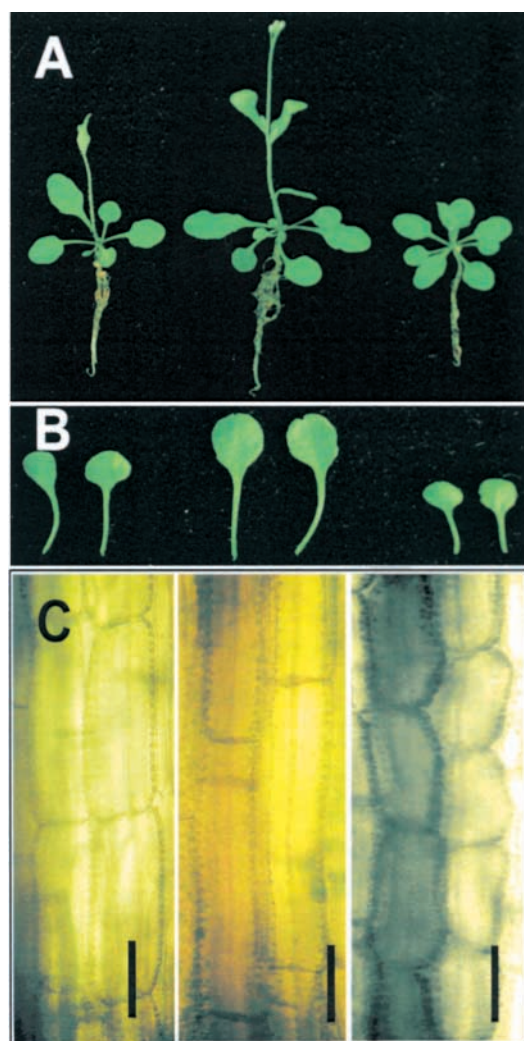


Figure 8. Comparison of the Growth of Inflorescence Stems and Leaf Petioles in Wild-Type and Transgenic Arabidopsis Plants.

Twenty-five-day-old Arabidopsis plants (**A**) and leaf petioles (**B**), and light micrographs of the cortical cells in longitudinal sections of leaf petioles (**C**). Wild-type Col-0 (left), *AtsPLA₂β*-overexpressing T3 transgenic line 1-1 (middle), and *AtsPLA₂β*-silenced T3 transgenic line C-5 (right) are shown. Bars = 100 μ m.

bending in all of the transgenic lines were significantly different from the rate observed in wild-type plants. The time required to bend by 90° was >30 min longer in transgenic plants than in wild-type plants. Although wild-type stems continued to bend past 90°, *sPLA₂*-overexpressing transgenic plants, after resuming vertical growth, did not bend further during the 4-h period. The dark-grown hypocotyls of *AtsPLA₂β*-overexpressing or -silenced transgenic Arabidopsis plants also showed altered gravitropic responses, whereas root gravitropism was not altered significantly.

The reason for the altered gravitropic response in shoots and hypocotyls, but not in roots, is not clear. One possible explanation is that in roots, *AtsPLA₂β* expression is restricted to the vascular tissues and undetectable in the cortical and endodermal cells, where perception and signaling for gravitropic response may occur. For the altered shoot gravitropism, we believe that upregulation or downregulation of *AtsPLA₂* activity disrupts the asymmetric growth of hypocotyls and inflorescence stems. Because the asymmetric growth of the organs probably is mediated by the differential distribution of auxin in response to gravity stimulation (Kiss, 2000; Kato et al., 2002; Moore, 2002), we propose that *AtsPLA₂β* may mediate auxin-induced differential cell elongation and that *AtsPLA₂β*-mediated differential cell elongation was interfered with by the upregulation and downregulation of *AtsPLA₂β* expression. The auxin-dependent elongation of hypocotyl segments is inhibited by treatment with *PLA₂* inhibitors (Scherer and Arnold, 1997). Auxin induces a rapid increase of FFA, LPC, and LPE levels, suggesting the stimulation of *PLA₂* activity by auxin (Paul et al., 1998). We observed that *AtsPLA₂β* expression was activated rapidly by auxin treatment. Moreover, expression was stimulated in the curving region of inflorescence stems after horizontal gravistimulation, suggesting the gravitropic response-specific induction of *AtsPLA₂β* expression. Based on these results, we propose that *AtsPLA₂β* is activated by auxin and mediates auxin-induced cell elongation and that differential cell elongation induced by auxin was interfered with by the upregulation and downregulation of *AtsPLA₂β* expression. However, the mechanisms by which *AtsPLA₂β* mediates auxin-induced differential cell elongation during shoot gravitropism remain to be elucidated.

Recent studies of the putative phosphatidic acid-preferring phospholipase A₁ (*PLA₁*) mutant of Arabidopsis, which exhibits normal root gravitropism but impaired shoot gravitropism, sug-

Table 3. Longitudinal Lengths of Epidermal and Cortical Cells in the Petioles and Inflorescence Stems of Transgenic Plants That Overexpress *AtsPLA₂β* or Silence *AtsPLA₂β* Expression Compared with Wild-Type Plants

Plant Type	Petiole Cell Length (μ m)		Stem Cell Length (μ m)	
	Epidermal	Cortical	Epidermal	Cortical
Wild Type	408.7 \pm 35.7	234.9 \pm 57.72	261.8 \pm 50.0	59.3 \pm 8.3
Overexpressing	568.7 \pm 164.1 ^a	354.9 \pm 60.56 ^b	405.9 \pm 70.8 ^b	84.3 \pm 4.8 ^b
RNAi silenced	273.5 \pm 43.9 ^b	125.7 \pm 37.14 ^b	225.5 \pm 35.7	38.1 \pm 7.6 ^b

Values shown are mean lengths \pm SD ($n = 20$).

^aMean values are statistically different ($P < 0.002$) from mean values in the wild type.

^bMean values are statistically different ($P < 0.0001$) from mean values in the wild type.

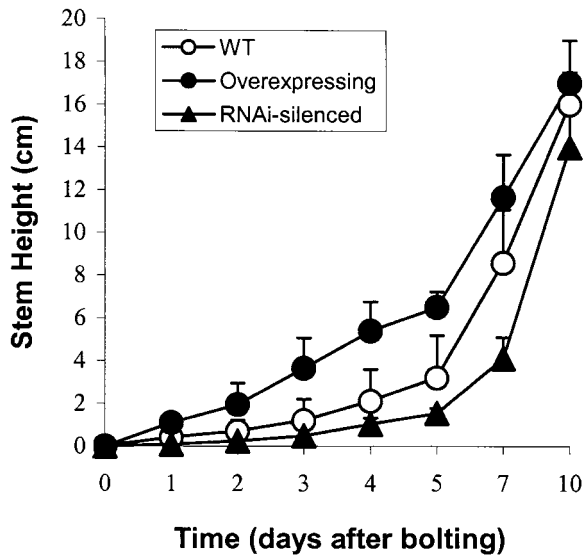


Figure 9. Time Course of Longitudinal Growth in the Inflorescence Stems of Wild-Type and Transgenic Arabidopsis Plants.

Data for wild-type (WT) plants (Col-0; open circles), *AtsPLA₂β*-overexpressing transgenic plants (T3 1-1 line; closed circles), and *AtsPLA₂β*-silenced plants (T3 C-5 line; closed triangles). The vertical error bars represent SD values ($n = 20$).

gested that the putative PLA₁ regulates vacuolar membrane structure and fluidity, forms the gravity-sensing signal, or influences downstream signals in the gravitropic sensing pathway of Arabidopsis shoots (Kato et al., 2002; Morita et al., 2002). This report suggests that lysophospholipids and free fatty acids perform certain cellular roles, especially in shoot gravitropism but not in root gravitropism. It should be noted, however, that PLA₂ and PLA₁ act at different acyl positions in glycerophospholipids, resulting in the generation of different lysophospholipids, and they are different in their cellular localizations. Thus, the cellular role of *AtsPLA₂β* may differ from that of the putative *AtsPLA₁*.

Consistent with the presence of an N-terminal signal sequence, *AtsPLA₂β* is secreted into the cell wall/extracellular space, where the signaling process for cell wall acidification may occur. The protein appears to be localized selectively to what might have been the newly formed cell plates. Lysophospholipids, the enzymatic products of PLA₂, activate a protein kinase that is involved in the acidification of cell walls by activating a H⁺ pump (Palmgren and Sommarin, 1989). LPC is involved in transient shifts in apoplastic and intracellular pH, which are essential steps in the gravitropic response (Scott and Allen, 1999; Kiss, 2000; Boonsirichai et al., 2002; Viehweger et al., 2002). *AtsPLA₂β* is transcribed in the cortical, vascular, and endodermal tissues of Arabidopsis stems and hypocotyls. Endodermal cells are known to be essential for the perception of gravity and the signaling pathway(s) involved in the gravitropic response (Boonsirichai et al., 2002; Kato et al., 2002; Morita et al., 2002). Cortical tissues are the sites at which asymmetric growth occurs between the upper and lower parts of responding organs. Although various

enzymes, signal molecules such as Ca²⁺, calmodulin, and inositol 1,4,5-triphosphate, and pH change are known to be involved in the signal transduction that generates the gravitropic response (Perera et al., 1999; Scott and Allen, 1999; Fasano et al., 2001; Kato et al., 2002), the signaling mechanisms between auxin and these proteins, signal molecules, or pH change in the gravitropic response have not been elucidated. Our study suggests that *AtsPLA₂β* regulates the process of cell elongation, possibly by activating key enzymes and signal molecules involved in cell wall acidification, and performs important roles in shoot gravitropism, possibly by mediating auxin-induced cell elongation.

METHODS

Materials and Reagents

1-Palmitoyl-2-¹⁴C-palmitoyl-phosphatidylcholine (PC), 1-palmitoyl-2-¹⁴C-linoleoyl-PC, and 1,2-¹⁴C-dipalmitoyl-PC were purchased from Amersham Pharmacia Biotech. All other chemicals were purchased from Sigma unless stated otherwise. An *Arabidopsis thaliana* cDNA library constructed in YESTrp2 (Invitrogen, Carlsbad, CA) was obtained from Soo Young Kim (Kumho Life and Environmental Science Laboratory, Gwangju, Korea).

Cloning of an sPLA₂ cDNA from Arabidopsis

Using the previously described N-terminal amino acid sequence of an elm PLA₂ (Stahl et al., 1998) as a query, we identified a related sequence in the Arabidopsis ecotype Columbia (Col-0) database (AtDB Stanford University; <http://genome-www.stanford.edu/Arabidopsis/>). Two PLA₂-specific oligonucleotides (5'-TCGCACTTCATTGATGCG-3' and 5'-TCATAGCTCTGTTTTTCATATCATTACCT-3') were used in combination with the T3 and T7 promoter-specific primers to isolate partial PLA₂ sequences from a cDNA library. The PCR contained 6 pmol of each primer and 1 unit of ExTaq polymerase (Pan Vera, Madison, WI) and consisted of 35 cycles of 94°C for 30 s, 60°C for 30 s, and 72°C for 1 min. Amplified products were isolated from a 0.8% (w/v) agarose gel and cloned into pGEM-T (Promega) for sequencing using the dideoxy-Sanger method, which is based on extension of oligonucleotide primers by DNA polymerase. The complete sequence of the Arabidopsis sPLA₂ gene was derived from the overlapping partial sequences.

Expression of Premature and Mature *AtsPLA₂β* Proteins in *Escherichia coli*

To obtain the complete coding regions of the putative Arabidopsis PLA₂ and to express the encoded proteins in *E. coli*, their cDNAs were amplified with the oligonucleotides 5'-GGATCCCATGATGTTTCGCACTTC-ATTGA-3' (forward), and 5'-CTCGAGTAGCTCTGTTTTTCATATCATTACCTAATTG-3' (reverse) using the same cycling program described above. The amplified cDNAs were cloned into the expression vector pET-40b(+) (Novagen, Madison, WI). The cloned product was introduced into BL21(DE3) PLYs cells (Novagen) to express the unprocessed form of *AtsPLA₂β* with the signal peptide fused to the C terminus of DsbC in pET-40b(+). Two milliliters of Luria-Bertani medium containing 150 μg/mL ampicillin was inoculated with a single colony from the BL21(DE3) transformation, and the culture was grown at 37°C overnight. Fifty microliters of the overnight culture was added to 500 mL of Luria-Bertani medium and grown at 37°C for 3 h. Overexpression of the fusion protein

then was induced by adding isopropylthio- β -galactoside (1 mM final concentration). The cells were incubated at 27°C for 2 h and harvested by centrifugation (5 min at 3000g). The cell pellet was resuspended in 1 mL of STE buffer (50 mM Tris-HCl, pH 8.0, 150 mM NaCl, 2 mM EDTA, and 1% Triton X-100) containing 0.25 M phenylmethylsulfonyl fluoride and sonicated briefly. The solution then was centrifuged for 5 min at 20,000g, the resulting supernatant was purified with the His-Bind purification kit (Novagen), and the levels of expression were monitored with the S-Tag rapid assay kit (Novagen).

To obtain the recombinant sPLA₂ protein without the signal peptide (mature form), cDNA was amplified with the oligonucleotides 5'-GGATCC-CGAGGAGTGACAAGAAGTTCATTG-3' (forward) and 5'-CTCGAG-TAGCTCTGTTTTTCATATCATTACCTAATTG-3' (reverse) and ligated to pET40b(+). The mature form of AtsPLA₂ β was overexpressed in BL21(DE3) PLys cells as its C-terminal fusion with DsbC and purified as described above. The free mature form of AtsPLA₂ β was released from the fusion protein with the S-Tag rEK purification kit (Novagen). For protein gel blot analysis, protein extracts were mixed with loading buffer, heated at 95°C for 3 min, and loaded onto a 12% (w/v) SDS-PAGE gel. After electrophoresis, proteins were stained with Coomassie Brilliant Blue R 250.

Assays of PLA₂ Activity

PLA₂ activity was measured as the release of radioactive lysophosphatidylcholine (LPC) and free fatty acid (FFA) from the substrate 1,2-¹⁴C-dipalmitoyl-PC. Standard enzyme assay mixtures contained 50 mM Tris-HCl, pH 8.0, 10 mM CaCl₂, 0.05% (v/v) Triton X-100, 20 μ L of the substrate, and 20 μ L of PLA₂ extract in a total volume of 200 μ L. The substrate was prepared by mixing radioactive PC (1.0 μ Ci, 108 mCi/mmol) with 2 μ mol of unlabeled 1-palmitoyl-2-linoleoyl-PC (Avanti Polar Lipids, Alabaster, AL) in chloroform, drying the mixture under a stream of N₂, and emulsifying it in 1 mL of water by sonication at room temperature. The reactions were incubated in a shaking water bath at 30°C for 30 min, 90 min, or 2.5 h and terminated by the addition of 750 μ L of chloroform:methanol (1:2, v/v) followed by 200 μ L of chloroform and 200 μ L of KCl (2 M). After vortexing, the chloroform and aqueous phases were separated by centrifugation at 12,000g for 5 min. The chloroform phase was dried, dissolved in chloroform, and spotted onto a thin layer chromatography plate (Silica Gel G), which was developed with chloroform:methanol:NH₄OH:water (65:39:4:4). Lipids on the plates were visualized by brief exposure to iodine vapor. The spots corresponding to the lipid standards FFA and LPC then were scraped into vials, and their radioactivities were determined by standard scintillation counting.

RNA Gel Blot and Reverse Transcriptase-Mediated PCR Analyses

Total RNA was isolated from Arabidopsis ecotype Col-0 roots, stems, leaves, flowers, and siliques using RNA Isolator (GIBCO) and treated with DNase RQ1 (Promega) to remove residual DNA. RNA gel blot analysis was performed as described (Ryu and Wang, 1995). Relative reverse transcriptase-mediated (RT) PCR was performed using an endogenous standard with the QuantumRNA 18S kit (Ambion, Austin, TX). Two micrograms of total RNA or 150 ng of mRNA isolated from total RNA was used as the template for each RT reaction. Random decamers were used as primers for the RT reactions. As an endogenous standard, an 18S rRNA or ubiquitin cDNA fragment was amplified concomitantly with PLA₂. The conditions for the PCR were 20 to 35 cycles of 94°C for 30 s, 65°C for 30 s, and 72°C for 30 s. Amplified products were separated on a 1.4% (w/v) agarose gel, stained with ethidium bromide, and visualized by UV light. Candidate PLA₂ DNA fragments were isolated from the gel, and their sequences were confirmed by dideoxy-Sanger sequence analysis.

Promoter Constructs, Plant Transformation, and Analysis of Transgenic Plants

Sequences beginning 699 or 469 bp upstream of the ATG start codon of AtsPLA₂ β were amplified by PCR from Arabidopsis genomic DNA as EcoRI-BglII fragments. 5'-oligonucleotide primers were 5'-GAATTC-GAGACAACAACAACCAGGTCG-3' and 5'-GAATTCACAAAAGTTTAA-TATCTGTTCAC-3', corresponding to -699 to -678 and -469 to -447, respectively. The 3' end primer (5'-AGATCTATCGTCGTCGTCGTCG-3') was the reverse complement to nucleotides -13 to +5 with an added BglII site. The two 5' fragments were used to replace the *Cauliflower mosaic virus* (CaMV) 35S promoter sequence of pCambia1303, and the binary plasmids were transferred to *Agrobacterium tumefaciens* EHA105 by the freeze-thaw method. Arabidopsis plants were transformed by the in planta method (Clough and Bent, 1998). Twenty-six independent T3 transgenic lines were generated with each 699- and 469-bp promoter construct on 1 \times Murashige and Skoog (1962) salts (Sigma, St. Louis, MO), and 0.8% (w/v) agar medium containing 50 mg/L hygromycin. β -Glucuronidase (GUS) activity was localized according to a described procedure (Jefferson et al., 1987). The tissue-specific patterns of GUS staining were similar in all transgenic plants carrying either of the two promoter constructs. Microscopic analyses with cross-sections were performed using an Olympus BX51 microscope (Tokyo, Japan) according to Hall and Cannon (2002).

Subcellular Localization Analysis of AtsPLA₂ β

The green fluorescent protein (GFP) was fused in frame to the C terminus of unprocessed AtsPLA₂ or the signal peptide. The fusion construct was cloned into the BamHI site of the vector pBI221 (Clontech, Palo Alto, CA) and introduced into onion epidermal cells using a helium biolistic particle delivery system (Bio-Rad) as described by Shieh et al. (1993). After incubation for 24 or 48 h at 23°C, the subcellular distribution of GFP was examined by fluorescence microscopy (Olympus). A pBI221 construct containing GFP but without PLA₂ was included as a control for subcellular localization.

Transgenic Plants that Overexpress AtsPLA₂ β or Silence AtsPLA₂ β Expression

To generate AtsPLA₂ β -overexpressing transgenic Arabidopsis plants (Col-0 ecotype), AtsPLA₂ β cDNA (441 bp) containing the complete open reading frame was cloned into the BamHI and NruI sites of the binary plant transformation vector pBI121 between the CaMV 35S promoter and the nopaline synthase terminator. To make the DNA construct for RNA interference-mediated silencing of the AtsPLA₂ β gene, partial cDNAs (99 bp) corresponding to the PA2c domain were amplified with two primer pairs: 5'BamHI (5'-CTCTTGGATCCCCGATATGGGAAGTATT-GTGGG-3') and 3'ClaI (5'-CCGTTATCGATAACACAATGGTCATGG-ATCTTAC-3'), and 5'XhoI (5'-CTCTTCTCGAGCGATATGGGAAGTATT-GTGGG-3') and 3'KpnI (5'-CCGTTGGTACCAACACAATGGTCATGG-ATCTTAC-3').

The BamHI-ClaI fragment was subcloned into an intron-spliced hairpin RNA vector, pKANNIBAL (Commonwealth Scientific and Industrial Research Organization Plant Industry, Canberra, Australia), in the forward orientation, and then the XhoI-KpnI fragment was integrated into the resulting vector as described above in the reverse orientation. The de novo-constructed vector was digested with NotI and subcloned into pART27 (Gleave, 1992). The construct was transformed into *A. tumefaciens* strain GV3101 using the freeze-thaw method described by Xie et al. (2001). *A. tumefaciens*-mediated in planta transformation of Arabidopsis was performed according to the method of Bechtold and Pelletier (1998). Transgenic plants were selected on 1 \times Murashige and Skoog

(1962) salts (Sigma) and 0.8% (w/v) agar plus kanamycin (100 mg/L), transferred to soil, and grown to maturity. RT-PCR assays of transgenic plants were performed as described above. To measure PLA₂ activity, total proteins were extracted in an extraction buffer (50 mM Tris-HCl, pH 7.0, 10 mM KCl, 10 mM NaF, 1 mM Na₂VO₄, 0.1 mM phenylmethylsulfonyl fluoride, 1 μg/mL leupeptin, and 1 μg/mL pepstatin) and assayed as described above.

Gravitropic Response Assays of Inflorescence Stems, Hypocotyls, and Roots

To examine the gravitropic responses of inflorescence stems, pots of soil-grown *Arabidopsis* plants with primary stems 6 to 10 cm in length were placed horizontally in the dark at 23°C. Because the stem elongation rates of wild-type and *AtsPLA₂β*-transgenic plants were different, the heights of plant samples were synchronized by adjusting the dates that seeds were sown. As described by Kato et al. (2002), the curvature of the stems was defined as the angle formed between the direction of apical growth and the horizontal baseline. Approximately 30 individual plants from each of three independent transgenic lines were examined four times.

To determine the gravitropic responses of hypocotyls and roots, seeds were surface-sterilized, plated on Murashige and Skoog (1962) agar plates, and vernalized in the dark at 4°C for 3 days. Because the growth rates of hypocotyls and roots in the dark were not evidently different among the transgenic and wild-type plants, we did not need to synchronize them. The plates then were wrapped with aluminum foil and placed vertically in a tissue culture room at 22°C for 3 days for seedling growth in the dark. Gravitropism was provided by turning the plates through 90°. Digital images were taken to measure the change in the orientation of the main root axis at 26 and 48 h after gravistimulation.

Upon request, materials integral to the findings presented in this publication will be made available in a timely manner to all investigators on similar terms for noncommercial research purposes. To obtain materials, please contact Stephen B. Ryu, sbryu@hanmail.net.

Accession Numbers

The GenBank accession number for *AtsPLA₂β* is AF541915. The GenBank accession numbers for the sequences shown in Figure 1 are AJ238116 (putative rice sPLA₂ type I), AJ238117 (putative rice sPLA₂ type II), AF064732 (putative carnation sPLA₂), and BAA36404 (cobra venom sPLA₂). Accession numbers for the other putative sPLA₂ cDNAs mentioned are as follows: AI164389 (*Populus*); AI487873 and BG127198 (tomato); BF275891 (cotton); AW289670 (pine); AI522932, AW318251, BE802011, and BG045671 (soybean); and C27540, D47653, D47724, and D49050 (rice).

ACKNOWLEDGMENTS

We thank Jed Doelling and Jung Mook Kim for their critical readings of the manuscript. This work was partially supported by a grant (R01-2000-000-00128-0 to S.B.R. and J.S.S.) from the Basic Research Program of the Korea Science and Engineering Foundation, a grant (M103KD010059-03K0401-05910 to S.B.R.) from the Plant Diversity Research Center of the 21st Century Frontier Research Program funded by the Ministry of Science and Technology of the Korean government, and a grant (CG1212 to J.S.S.) from the Crop Functional Genomics Center of the 21st Century Frontier Research Program funded by the Ministry of Science and Technology. We also wish to acknowledge that our studies on the cloning and characterization of PLA₂ genes began at the University of Wisconsin, Madison. Using the published N-terminal amino acid sequence of a purified Elm PLA₂ as query, we identified two related se-

quences in *Arabidopsis* ecotype database. We cloned and characterized a PLA₂ cDNA from *Arabidopsis* and named it *AtsPLA₂α*. Using the deduced amino acid sequence of this gene as query and a full search of the *Arabidopsis* genome, we identified the presence of multiple sPLA₂ genes, *At2g06925*, *At4g29460*, and *At4g29470*, which we named as *AtsPLA₂β*, *AtsPLA₂γ*, and *AtsPLA₂δ*, respectively. The present study reports on the cloning and characterizing of the second gene, which resulted from the continued collaboration between J.P.P. and S.B.R. after S.B.R. moved to Kumho Life and Environmental Science Laboratory in Korea.

Received June 6, 2003; accepted July 2, 2003.

REFERENCES

- Bechtold, N., and Pelletier, G. (1998). In planta *Agrobacterium*-mediated transformation of adult *Arabidopsis thaliana* plants by vacuum infiltration. *Methods Mol. Biol.* **82**, 259–266.
- Boonsirichai, K., Guan, C., Chen, R., and Masson, P.H. (2002). Root gravitropism: An experimental tool to investigate basic cellular and molecular processes underlying mechanosensing and signal transmission in plants. *Annu. Rev. Plant Biol.* **53**, 421–447.
- Brightman, A.O., Zhu, X.Z., and Morrè, D.J. (1991). Activation of plasma membrane NADH oxidase activity by products of phospholipase A. *Plant Physiol.* **96**, 1314–1320.
- Chapman, K.D. (1998). Phospholipase activity during plant growth and development and in response to environmental stress. *Trends Plant Sci.* **3**, 419–426.
- Clough, S.J., and Bent, A.F. (1998). Floral dip: A simplified method for *Agrobacterium*-mediated transformation of *Arabidopsis thaliana*. *Plant J.* **16**, 735–743.
- Creelman, R.A., and Mullet, J.E. (1997). Biosynthesis and action of jasmonates in plants. *Annu. Rev. Plant Physiol. Plant Mol. Biol.* **48**, 355–381.
- Farag, K.M., and Palta, J.P. (1993a). Use of lysophosphatidylethanolamine, a natural lipid, to retard tomato leaf and fruit senescence. *Physiol. Plant.* **87**, 515–524.
- Farag, K.M., and Palta, J.P. (1993b). Use of natural lipids to accelerate ripening and enhance storage life of tomato fruit with and without ethephon. *Horttechnology* **3**, 62–65.
- Fasano, J.M., Swanson, S.J., Blancaflor, E.B., Dowd, P.E., Kao, T., and Gilroy, S. (2001). Changes in root cap pH are required for the gravity response of the *Arabidopsis* root. *Plant Cell* **13**, 907–922.
- Gleave, A.P. (1992). A versatile binary vector system with a T-DNA organizational structure conducive to efficient integration of cloned DNA into the plant genome. *Plant Mol. Biol.* **20**, 1203–1207.
- Hall, Q., and Cannon, M.C. (2002). The cell wall hydroxyproline-rich glycoprotein RSH is essential for normal embryo development in *Arabidopsis*. *Plant Cell* **14**, 1161–1172.
- Jefferson, R.A., Kavanagh, T.A., and Bevan, M.W. (1987). GUS fusions: β-Glucuronidase as a sensitive and versatile gene fusion marker in higher plants. *EMBO J.* **6**, 3901–3907.
- Kato, T., Morita, M.T., Fukaki, H., Yamauchi, Y., Uehara, M., Niihama, M., and Tasaka, M. (2002). SGR2, a phospholipase-like protein, and ZIG/SGR4, a SNARE, are involved in the shoot gravitropism of *Arabidopsis*. *Plant Cell* **14**, 33–46.
- Kaur, N., and Palta, J.P. (1997). Postharvest dip in lysophosphatidylethanolamine, a natural phospholipid, may prolong vase-life of snapdragon flowers. *HortScience* **32**, 888–890.
- Kim, J.Y., Chung, Y.S., Ok, S.H., Lee, S.G., Chung, W.I., Kim, I.Y., and Shin, J.S. (1999). Characterization of the full-length sequences of phospholipase A₂ induced during flower development. *Biochim. Biophys. Acta* **1489**, 389–392.

- Kiss, J.Z.** (2000). Mechanisms of the early phases of plant gravitropism. *Crit. Rev. Plant Sci.* **19**, 551–573.
- Lee, S.M., Suh, S., Kim, S., Crain, R.C., Kwak, J.M., Nam, H.G., and Lee, Y.S.** (1997). Systemic elevation of phosphatidic acid and lysophospholipid levels in wounded plants. *Plant J.* **12**, 547–556.
- Li-Stiles, B., Lo, H.-H., and Fischer, S.M.** (1998). Identification and characterization of several forms of phospholipase A₂ in mouse epidermal keratinocytes. *J. Lipid Res.* **39**, 569–582.
- Martiny-Baron, G., and Scherer, G.F.E.** (1989). Phospholipid-stimulated protein kinase in plants. *J. Biol. Chem.* **264**, 18052–18059.
- May, C., Preisig-Müller, R., Höhne, M., Gnau, P., and Kindl, H.** (1998). A phospholipase A₂ is transiently synthesized during seed germination and localized to lipid bodies. *Biochim. Biophys. Acta* **1393**, 267–276.
- Moore, I.** (2002). Gravitropism: Lateral thinking in auxin transport. *Curr. Biol.* **12**, R452–R454.
- Morita, M.T., Kato, T., Nagafusa, K., Saito, C., Ueda, T., Nakano, A., and Tasaka, M.** (2002). Involvement of the vacuoles of the endodermis in the early process of shoot gravitropism in Arabidopsis. *Plant Cell* **14**, 47–56.
- Munnik, T., Irvine, R.F., and Musgrave, A.** (1998). Phospholipid signaling in plants. *Biochim. Biophys. Acta* **1389**, 222–272.
- Murashige, T., and Skoog, F.** (1962). A revised medium for rapid growth and bioassays with tobacco tissue culture. *Physiol. Plant.* **15**, 473–497.
- Narváez-Vásquez, J., Florin-Christensen, J., and Ryan, C.A.** (1999). Positional specificity of a phospholipase A activity induced by wounding, systemin, and oligosaccharide elicitors in tomato leaves. *Plant Cell* **11**, 2249–2260.
- Palmgren, M.G., and Sommarin, M.** (1989). Lysophosphatidylcholine stimulates ATP dependent proton accumulation in isolated oat root plasma membrane vesicles. *Plant Physiol.* **90**, 1009–1014.
- Paul, R.U., Holk, A., and Scherer, G.F.E.** (1998). Fatty acids and lysophospholipids as potential second messengers in auxin action: Rapid activation of phospholipase A₂ activity by auxin in suspension-cultured parsley and soybean cells. *Plant J.* **16**, 601–611.
- Perera, I.Y., Heilmann, I., and Boss, W.F.** (1999). Transient and sustained increases in inositol 1,4,5-trisphosphate precede the differential growth response in gravistimulated maize pulvini. *Proc. Natl. Acad. Sci. USA* **96**, 5838–5843.
- Pohnert, G.** (2002). Phospholipase A₂ activity triggers the wound-activated chemical defense in the diatom *Thalassiosira rotula*. *Plant Physiol.* **129**, 103–111.
- Roos, W., Dordschbal, B., Steighardt, J., Hieke, M., Weiss, D., and Saalbach, G.** (1999). A redox-dependent, G-protein-coupled phospholipase A of the plasma membrane is involved in the elicitation of alkaloid biosynthesis in *Eschscholtzia californica*. *Biochim. Biophys. Acta* **1448**, 390–402.
- Ryu, S.B., Karlsson, B.H., Özgen, M., and Palta, J.P.** (1997). Inhibition of phospholipase D by lysophosphatidylethanolamine, a lipid-derived senescence retardant. *Proc. Natl. Acad. Sci. USA* **94**, 12717–12721.
- Ryu, S.B., and Wang, X.** (1995). Expression of phospholipase D during castor bean leaf senescence. *Plant Physiol.* **108**, 713–719.
- Scherer, G.F.E.** (1996). Phospholipid signalling and lipid-derived second messengers in plants. *Plant Growth Regul.* **18**, 125–133.
- Scherer, G.F.E., and Arnold, B.** (1997). Inhibitors of animal phospholipase A₂ enzymes are selective inhibitors of auxin-dependent growth: Implications for auxin-induced signal transduction. *Planta* **202**, 462–469.
- Scott, A.C., and Allen, N.S.** (1999). Changes in cytosolic pH within Arabidopsis root columella cells play a key role in the early signaling pathway for root gravitropism. *Plant Physiol.* **121**, 1291–1298.
- Scott, D.L., White, S.P., Otwinowski, Z., Yuan, W., Gelb, M.H., and Sigler, P.B.** (1990). Interfacial catalysis: The mechanism of phospholipase A₂. *Science* **250**, 1541–1546.
- Senda, K., Doke, N., and Kawakita, K.** (1998). Effect of mastoparan on phospholipase A₂ activity in potato tubers treated with fungal elicitor. *Plant Cell Physiol.* **39**, 1080–1086.
- Shieh, M.W., Wessler, S.R., and Raikhel, N.V.** (1993). Nuclear targeting of the maize R protein requires two nuclear localization sequences. *Plant Physiol.* **101**, 353–361.
- Six, D.A., and Dennis, E.A.** (2000). The expanding superfamily of phospholipase A₂ enzymes: Classification and characterization. *Biochim. Biophys. Acta* **1488**, 1–19.
- Ståhl, U., Banas, A., and Stymne, S.** (1995). Plant microsomal acyl hydrolases have selectivities for uncommon fatty acids. *Plant Physiol.* **107**, 953–962.
- Ståhl, U., Ek, B., and Stymne, S.** (1998). Purification and characterization of a low-molecular-weight phospholipase A₂ from developing seeds of elm. *Plant Physiol.* **117**, 197–205.
- Ståhl, U., Lee, M., Sjö Dahl, S., Archer, D., Cellini, F., Ek, B., Iannaccone, R., MacKenzie, D., Semeraro, L., Tramontano, E., and Stymne, S.** (1999). Plant low-molecular-weight phospholipase A₂s (PLA₂s) are structurally related to the animal secretory PLA₂s and are present as a family of isoforms in rice (*Oryza sativa*). *Plant Mol. Biol.* **41**, 481–490.
- Valentin, E., and Lambeau, G.** (2000). Increasing molecular diversity of secreted phospholipases A₂ and their receptors and binding proteins. *Biochim. Biophys. Acta* **1488**, 59–70.
- Viehweger, K., Dordschbal, B., and Roos, W.** (2002). Elicitor-activated phospholipase A₂ generates lysophosphatidylcholines that mobilize the vacuolar H⁺ pool for pH signaling via the activation of Na⁺-dependent proton fluxes. *Plant Cell* **14**, 1509–1525.
- White, S.P., Scott, D.S., Otwinowski, Z., Gelb, M.H., and Sigler, P.B.** (1990). Crystal structure of cobra-venom phospholipase A₂ in a complex with a transition-state analogue. *Science* **250**, 1560–1563.
- Xie, M., He, Y., and Gan, S.** (2001). Bidirectionalization of polar promoters in plants. *Nat. Biotechnol.* **19**, 677–679.
- Yi, H., Park, D., and Lee, Y.** (1996). In vivo evidence for the involvement of phospholipase A and protein kinase in the signal transduction pathway for auxin-induced corn coleoptile elongation. *Physiol. Plant.* **96**, 359–368.
- Zhang, Y., Lemasters, J., and Herman, B.** (1999). Secretory group IIA phospholipase A₂ generates anti-apoptotic survival signals in kidney fibroblasts. *J. Biol. Chem.* **274**, 27726–27733.